Available online at www.sciencedirect.com
ScienceDirect
Physics Letters A 362 (2007) 489–493
PHYSICS LETTERS A
www.elsevier.com/locate/pla

Magnetoresistance effect in a both magnetically and electrically modulated nanostructure

Mao-Wang Lu, Guo-Jian Yang *

Department of Physics, Beijing Normal University, Beijing 100875, People's Republic of China

Received 9 September 2006; received in revised form 18 October 2006; accepted 23 October 2006

Available online 10 November 2006

Communicated by J. Flouquet

Abstract

We propose a magnetoresistance device in a both magnetically and electrically modulated two-dimensional electron gas, which can be realized experimentally by the deposition, on the top and bottom of a semiconductor heterostructure, of two parallel metallic ferromagnetic strips under an applied voltage. It is shown that a considerable magnetoresistance effect can be achieved in such a device due to the significant transmission difference for electrons through parallel and antiparallel magnetization configurations. It is also shown that the magnetoresistance ratio depends strongly on the applied voltage to the stripe in the device. These interesting properties may provide an alternative scheme to realize magnetoresistance effect in hybrid ferromagnetic/semiconductor nanosystems, and this system may be used as a voltage-tunable magnetoresistance device.

PACS: 73.40.-c; 75.75.+a; 72.20.-i; 73.23.-b

1. Introduction

A large magnetoresistance (MR) effect, especially the giant magnetoresistance (GMR) effect [1], has been searched for during the past several decades. At present, the MR effect has given rise to a lot of significant practical applications in magnetic information storage [2], including ultrasensitive magnetic field sensors, read heads, random access memories, and so on. Generally, the structures, where MR is observed, consist of ferromagnetic layers separated by thin non-magnetic layers. In such heterogeneous systems, GMR is characterized by a striking drop of the electric resistance when a external magnetic field switches the magnetization of adjacent magnetic layers from an antiparallel (AP) alignment to a parallel (P) one. For a specific GMR device, one hopes from the viewpoint of practical applications that the system possesses the high MR ratio under relatively low saturation magnetic field.

To obtain a large MR ratio, an attractive alternative is to use magnetic or superconducting microstructures on the surface of heterostructures containing a two-dimensional electron gas (2DEG). Microstructured ferromagnets or superconductors provide an inhomogeneous magnetic field which influences locally the motion of the electrons in the semiconductor. Nogaret et al. [3] demonstrated a MR effect in hybrid ferromagnetic and/or semiconductor devices at low temperature, and a MR ratio of up to $10^3\%$ at 4 K has been observed recently [4]. It was also reported that MR oscillations, due to the internal Landau band structure of a 2DEG system, can be observed in a periodic magnetic field [5].

More recently, a spin-independent MR effect have attracted considerable attention in a magnetically modulated 2DEG system [6–9]. Using the δ-function magnetic barriers on the two-dimensional electron gas (2DEG), a MR device was proposed by Zhai et al. [6]. It has been found that, although the average magnetic field of the structure is zero, this kind of system possesses very high MR ratio, and the MR effect makes no use of the spin degree of freedom distinct from the conventional MR devices. The MR effect in realistic case, where the exact magnetic profiles instead of the ideal δ-function magnetic barriers

* Corresponding author.
E-mail address: yangguojian2006@126.com (G.-J. Yang).

0375-9601/$ – see front matter
doi:10.1016/j.physleta.2006.10.058

were employed, was also studied [7]. Yang et al. [8] investigated the MR effect of 2DEG systems subjected to a periodically modulated magnetic field, and found that the MR ratio of such a periodically modulated system shows strong dependence on the space between the magnetic potentials and the number of periods.

In the Letter, we propose an alternative scheme to realize the MR effect, based on the magnetically and electrically modulated semiconductor nanostructures. By numerical calculations for realistic GaAs material system, we demonstrate that such a device does possess the considerable MR effect. Moreover, its MR ratio varies with the electric-barrier (EB) height, thus the considered system can be employed as a MR device with the MR ratio tunable by the EB.

2. Model and formulas

The system under consideration is a 2DEG formed usually in a modulation-doped semiconductor heterostructure, subject to modulation by a perpendicular magnetic field. This system can be experimentally realized [10] by depositing two ferromagnetic (FM) stripes on the top and bottom of a semiconductor heterostructure, as schematically depicted in Fig. 1(a). The in-plane magnetization of the FM layers creates an out-of-plane fringe magnetic field at both ends. This fringe field constitutes a nonhomogeneous magnetic barrier for electron transport within the 2DEG. The two FM stripes are assumed to be asymmetric in length, with a distance L between their right edges, and within this gap a negative voltage is applied directly to the 2DEG to induce further an EB. The two FM layers are also different in distance relative to the 2DEG: the distance of the upper FM layer is smaller than that of the FM layer at the bottom, which will result in the magnetic barriers produced by the two FM stripes with unidentical strengths (because the magnetic strength enhances with decreasing the distance of the FM stripe relative to the 2DEG) [11]. Making use of the modern nanotechnology such a system can be deliberately designed to fall short of the left-hand edges of the FM layers, so that the effects of fringe field there can be ignored. The magnetization directions of the FM stripes are assumed to be parallel in Fig. 1(a), and the resulting magnetic field and electrical potential profiles are presented schematically in Fig. 1(b). For simplicity, the magnetic and electric barriers can be approximated [12] as a delta function (solid curve) and square (dashed curve), respectively, in order to demonstrate the principle of operation of this device, as shown in Figs. 1(c) and 1(d). Here, Figs. 1(c) and 1(d) correspond to the parallel (P) and antiparallel (AP) configurations of two FM layers, respectively. The magnetic field can be expressed as $B_z(x) = [B_1\delta(x + \frac{L}{2}) - \chi B_2\delta(x - \frac{L}{2})]$, where B_1 and B_2 are the magnetic strengths of two δ-function barriers, L is their separation, and χ represents the magnetization configuration (± 1 or P/AP). Assume that the magnetic field provided by the FM stripe, $B_z(x)$, and the electric potential induced by the applied voltage to the metallic FM stripe, $U(x)$, are homogeneous in the y direction and vary only along the x axis. The motion of an electron in such a modulated 2DEG system in the (x, y) plane, can be described by the single-particle Hamiltonian

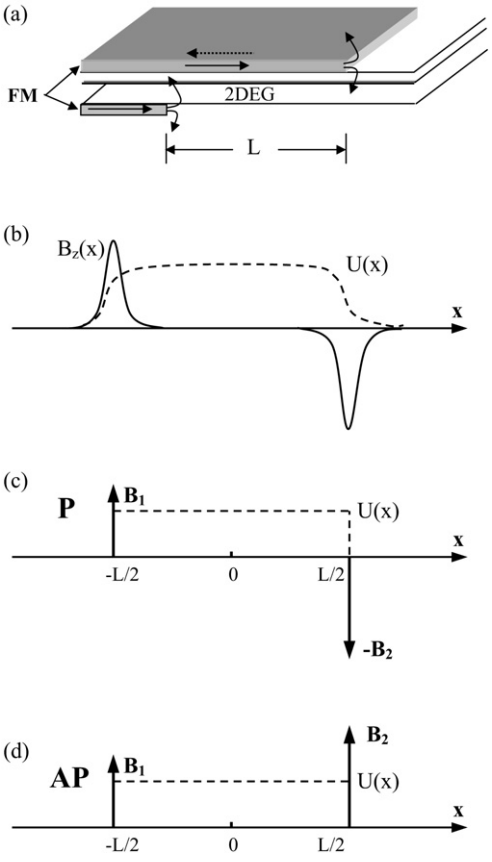

Fig. 1. (a) The schematic illustration of the MR device, where two metallic magnetic stripes under an applied voltage are placed on the top and bottom of a 2DEG. (b) Magnetic field and electrical potential profiles induced in the 2DEG. Magnetic–electric barrier models (c) and (d) exploited in this work correspond to the P and AP alignments, respectively.

$$H = \frac{p_x^2}{2m_e^*} + \frac{[p_y + (e/c)A_y(x)]^2}{2m_e^*} + \frac{eg^*}{2m_e}\frac{\sigma_z\hbar}{2c}B_z(x) + U(x), \tag{1}$$

where m_e^* is the effective mass, m_e is the free electron mass, (p_x, p_y) is the electron momentum, g^* is the effective Landé factor of the electron in the 2DEG, $\sigma_z = +1/-1$ for spin-up/down electrons, and the magnetic vector potential of the device can be written as $\vec{A} = [0, A_y(x), 0]$ in the Landau gauge, i.e.,

$$A_y(x) = \begin{cases} 0, & x < -L/2, \\ B_1, & -L/2 < x < +L/2, \\ B_1 - \chi B_2, & x > L/2 \end{cases} \tag{2}$$

which results in $B_z(x) = dA_y(x)/dx$. For convenience, we introduce two characteristic quantities, the cyclotron frequency $\omega_c = eB_0/cm^*$ and the magnetic length $l_B = \sqrt{c\hbar/eB_0}$. Thus, all the relevant quantities can be expressed as the dimensionless forms in terms of ω_c and l_B: the magnetic field $B_z(x) \to B_0 B_z(x)$, the magnetic vector potential $\mathbf{A}(x) \to B_0 l_B \mathbf{A}(x)$, the coordinate $x \to l_B x$, and the energy $E \to \hbar\omega_c E$ $(= E_0 E)$. In our calculation, we take $B_0 = 0.1$ T, which leads to the units $l_B = 81.3$ nm and $E_0 = 0.17$ meV for the GaAs system with $m_e^* = 0.067m_e$ and $g^* = 0.44$.

Because of the translational invariance of the system along the y direction, the total electronic wave-function can be written as $\Phi(x, y) = e^{ik_y y}\psi(x)$, where k_y is the wave-vector component in the y direction. Accordingly, the wave function $\psi(x)$ satisfies the following reduced one-dimensional (1D) Schrödinger equation

$$\left\{\frac{d^2}{dx^2} - \left[k_y + A_y(x)\right]^2 + 2\left[E - U(x) - \frac{m_e^* g^* \sigma_z}{4m_e} B_z(x)\right]\right\} \times \psi(x) = 0. \tag{3}$$

It is useful to introduce the effective potential $U_{\text{eff}}(x, k_y) = [k_y + A_y(x)]^2/2 + U(x) + m_e^* g^* \sigma_z B_z(x)/(4m_e)$. Clearly, this effective potential of the system depends strongly not only on the magnetic configuration $B_z(x)$, but also on the longitudinal wave vector k_y. The k_y-dependence renders the motion of electrons an essentially two-dimensional (2D) process as would be expected from the classical analogy. From the dependence of the U_{eff} on the magnetic profile $B_z(x)$, one can easily see that for the device presented in Fig. 1 when the P alignment [Fig. 1(c)] turns to the inverse [Fig. 1(d)], U_{eff} varies substantially. It is the dependence on the magnetic configuration of U_{eff} that results in the MR effect in the involving systems.

The reduced 1D Schrödinger equation (3) can be solved exactly in each region [13], where the wave function is expressed by the linear combination of plane wave. In the left and right regions of the device, the wave functions can be written as $\psi_{\text{left}}(x, y) = \exp(ik_y y)[\exp(ik_l x) + \gamma \exp(-ik_l x)]$, $x < -L/2$ and $\psi_{\text{right}}(x, y) = \tau \exp(ik_y y)\exp(ik_r x)$, $x > L/2$, where $k_l = \sqrt{2E - [A_{yl}(x) + k_y]^2}$, $k_r = \sqrt{2E - [A_{yr}(x) + k_y]^2}$, and γ/τ is the reflection/transmission amplitude. In the intermediate region, $-L/2 < x < L/2$, the wave function can be assumed as $\psi_{\text{in}}(x, y) = \exp(ik_y y)[C_1 \exp(ikx) + C_2 \exp(-ikx)]$, where $k = \sqrt{2[E - U(x)] - [B_1 + k_y]^2}$, as well as C_1 and C_2 are two unknown constants determined by using of the boundary conditions. Thus, one can readily obtain the transmission coefficient as $T(E, k_y) = \frac{k_r}{k_l}|\tau|^2$.

Furthermore, we can calculate the ballistic conductance at zero temperature from the well-known Landauer–Büttiker formula [14]

$$G(E_F) = G_0 \int_{-\pi/2}^{\pi/2} T(E_F, \sqrt{2E_F}\sin\theta)\cos\theta\, d\theta, \tag{4}$$

with θ the incident angle relative to the x direction. The conductance is presented in units of $G_0 = 2e^2 m_e^* v_F L_y/h^2$, where v_F is the Fermi velocity and L_y is the longitudinal length of the system.

For a MR device, its MR ratio usually has two kinds of definitions [6,9], i.e., MRR $= (G_{\text{P}} - G_{\text{AP}})/G_{\text{AP}}$ or $(G_{\text{P}} - G_{\text{AP}})/G_{\text{P}}$ and MMRR $= (G_{\text{P}} - G_{\text{AP}})/(G_{\text{P}} + G_{\text{AP}})$, where G_{P} and G_{AP} are the conductance for the parallel and antiparallel alignments, respectively. Obviously, the MR ratio calculated by the different definitions is distinct for some cases. In this work, we adopt the MMRR definition to study the MR effect.

Although the delta function $B_z(x)$ is locally infinite, the effect of the polarization $g^* m_e^* B_z(x)/m_e$ on the MR effect extend to the whole infinite space. But, the Zeeman coupling term on the MR depends on the quantity $g^* B m_e^*/4m_e$, which equals to 0.0369 for $B = 5$ and for GaAs. Comparing to other terms in U_{eff}, the absolute value of such a Zeeman term is much smaller. Therefore, the spin-dependent term plays a minor role in determining the transport properties [6] and will be ignored in the subsequent discussion [9].

3. Results and discussion

First of all, in Fig. 2 we plot the transmission coefficients for P and AP alignments versus the incident energy E for electrons with different wave vector $k_y = 0$ (solid curve), 1 (dashed curve), and -1 (dotted curve), where Figs. 2(a) and 2(b) correspond to the P and AP configurations, respectively. The structural parameters are chosen to be $B_1 = 1.0$, $B_2 = 3.0$, and $L = 3.0$, and the EB height is taken as $U = 4.0$, for both configurations. Apparently, there exists a remarkable discrepancy in the transmission for electron through P and AP configurations of the FM layers. For the P configuration, one can obviously see from Fig. 2(a) that there are several incomplete resonant peaks in low-energy region. This can be expected because for the considered wave vectors k_y the effective potential U_{eff} has a relatively symmetric barrier structure for the P configuration, where the process of electron motion is resonantly tunneling through the barrier. However, when the system switches from

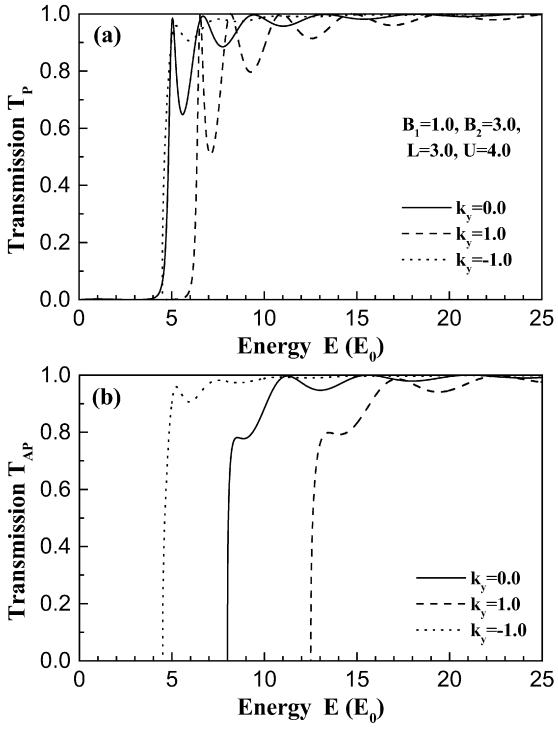

Fig. 2. (a) and (b) are the transmission coefficients for electrons tunneling through the P and AP configurations for a given EB height $U = 4$, respectively, where the structural parameters are chosen to be $B_1 = 1$, $B_2 = 3$, $L = 3$, and the wave vector components of electron are taken to be $k_y = 0$ (solid curve), 1 (dashed curve), and -1 (dotted curve).

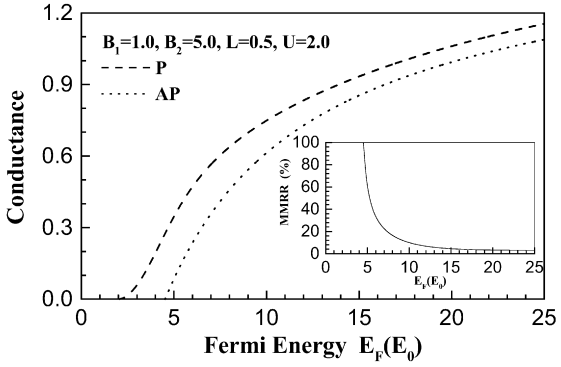

Fig. 3. The conductances G_{P} (dashed curve) and G_{AP} (dotted curve) of the P and AP alignments as a function of the Fermi energy E_F, where the conductances are in units of $G_0 = 2e^2 m_e^* v_F L_y/h^2$, the structural parameters are $B_1 = 1$, $B_2 = 5$, $L = 0.5$, and the EB height is $U = 2$. The inset gives the corresponding magnetoresistance ratio MMRR calculated as a function of the Fermi energy E_F.

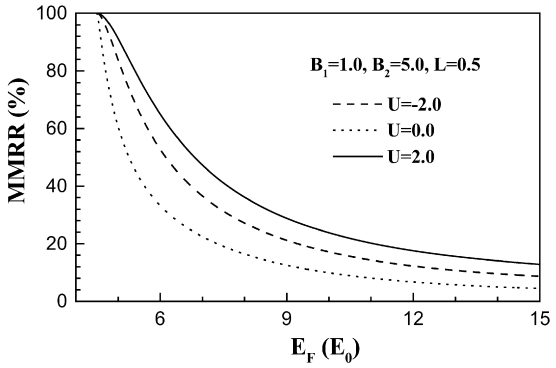

Fig. 4. The magnetoresistance ratio MMRR versus the Fermi energy E_F, where the device parameters are the same as in Fig. 3 but the EB height $U = 2$ (solid curve), -2 (dashed curve), and 0 (dotted curve).

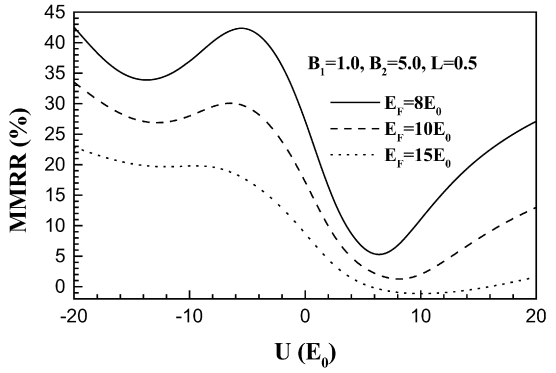

Fig. 5. The magnetoresistance ratio MMRR calculated as a function of the EB height U for the same device and parameters as in Fig. 3 at the Fermi energy $E_F = 8$ (solid curve), 10 (dashed curve), and 15 (dotted curve).

the P configuration to the AP configuration, one can see from Fig. 2(b) that the electron transmission is greatly altered because of the variation of the U_{eff} induced by the structure. The transmission curves shift towards high energy region and are greatly suppressed in contrast to the P configuration. Especially, the low-energy resonant peaks for the AP configuration disappears almost, because the change of the effective potential U_{eff} makes the electron transmission through AP configuration is incomplete.

The configuration-dependent transmission features demonstrated above should be reflected in the measurable quantity, the conductance G, which is obtained by integration of the transmission of electrons over the incident angle as in Eq. (4). Indeed, our calculated results also confirm this difference in the conductances G_{P} and G_{AP}. In Fig. 3 we present the conductances G_{P} (dashed curve) and G_{AP} (dotted curve) for the P and AP alignments versus the Fermi energy E_F, where the structural parameters are $B_1 = 1.0$, $B_2 = 5.0$, $L = 0.5$, $U = 2.0$ and the conductance is in units of G_0. The large suppression of the conductance G_{AP} is clearly seen due to the great reduction of the transmission coefficient T_{AP} in contrast to the P alignment. It is this large suppression on the conductance of the AP alignment that results in an evident MR effect in considered device. The inset of Fig. 3 shows that the magnetoresistance ratio MMRR as a function of the Fermi energy E_F for our considered system. A considerable MR effect can be evidently seen, especially in low-energy region. The MR effect changes its degree when the Fermi energy varies. In particular, it is striking that the MR ratio MMRR can be up to 100% at certain low-E_F, and the MMRR reduces with increasing the Fermi energy E_F.

Finally, we examine the influence of the electric barrier $U(x)$ induced by an applied voltage to the metallic FM stripe on the MR effect for the device as shown in Fig. 1(a). Fig. 4 shows the MR ratio MMRR versus the Fermi energy E_F for the device, where the structural parameters are the same as in Fig. 3 but $U(x) = 2.0$ (solid curve), -2.0 (dashed curve), and 0.0 (dotted curve). The MMRR shows a strong dependence on the electric potential $U(x)$ in considered energy range. The MMRR curve shifts to high Fermi energy region and its value is enhanced as the EB $U(x)$ is added, regardless of the EB sign. In order to demonstrate more clearly the role of the EB $U(x)$, in Fig. 5 we present the MR ratio MMRR as a function of the EB height $U(x)$ for three fixed Fermi energies: $E_F = 8$ (solid curve), 10 (dashed curve), and 15 (dotted curve). From these three MR ratio curves one can observe that the MMR may exhibit a drastic variation with changing the EB height. For the negative value of $U(x)$, the MR ratio MMRR is more large in contrast to the positive $U(x)$. Another observation from Fig. 5 is that, with increasing the Fermi energy the MR ratio MMRR curve is played down, and its value decreases evidently. These features attribute to the dependence of the effective potential U_{eff} (cf. Eq. (3) on the EB $U(x)$. At the same time, due to the EB produced by an applied voltage to the metallic FM stripe in the device, one can expect that the MR effect can be tuned by adjusting this applied voltage, which may result in a voltage-controlled MR device.

4. Conclusions

In summary, we propose a MR device in the 2DEG, which can be experimentally realized by the deposition, on the top and bottom of a conventional GaAs heterostructure, of two parallel metallic ferromagnetic stripes under an applied voltage. We have theoretically investigated the MR effect in this device, and

the role of the applied voltage is examined in detail. Our calculations show that, since there exists a evident tunneling difference in the P and AP configurations (especially the transmission suppression for the AP alignment), this device shows up a considerable MR effect. We have also exhibited that, the MR ratio is greatly influenced by the applied voltage to the FM stripe in the device, thus leading to a voltage-tunable MR device.

Acknowledgements

This work was supported by Scientific Research Fund of Hunan Provincial Education Department (Grant No. 04B053).

References

[1] M.N. Baibich, J.M. Broto, A. Fert, F. Nguyen Van Dau, F. Petroff, P. Etienne, G. Creuzet, A. Friederich, J. Chazelas, Phys. Rev. Lett. 61 (1988) 2472.
[2] G.A. Prinz, Science 282 (1998) 1660;
S.A. Wolf, D.D. Awschalom, R.A. Buhrman, J.M. Daughton, S. von Molnar, M.L. Roukes, A.Y. Chtchelkanova, D.M. Treger, Science 294 (2001) 1488.
[3] A. Nogaret, S. Carlton, B.L. Gallagher, P.C. Main, M. Henini, R. Wirtz, R. Newbury, M.A. Howson, S.P. Beaumont, Phys. Rev. B 55 (1997) R16037.
[4] N. Overend, A. Nogaret, B.L. Gallagher, P.C. Main, M. Henini, C.H. Marrows, M.A. Howson, S.P. Beaumont, Appl. Phys. Lett. 72 (1998) 1724.
[5] K.W. Edmonds, B.L. Gallagher, P.C. Main, N. Overend, R. Wirtz, A. Nogaret, M. Henini, C.H. Marrows, B.J. Hickey, S. Thoms, Phys. Rev. B 64 (2001) 041303.
[6] F. Zhai, Y. Guo, B.L. Gu, Phys. Rev. B 66 (2002) 125305.
[7] M.W. Lu, L.D. Zhang, J. Phys.: Condens. Matter 15 (2003) 1267.
[8] X.D. Yang, R.Z. Wang, Y. Guo, W. Yang, D.B. Yu, B. Wang, H. Yan, Phys. Rev. B 70 (2004) 115303.
[9] G. Papp, F.M. Peeters, J. Phys.: Condens. Matter 16 (2004) 8275;
G. Papp, F.M. Peeters, Physica E 25 (2005) 339;
G. Papp, F.M. Peeters, J. Appl. Phys. 100 (2006) 043707.
[10] V. Kubrak, F. Rahman, B.L. Gallagher, P.C. Main, M. Henini, C.H. Marrows, M.A. Howson, Appl. Phys. Lett. 74 (1999) 2507;
T. Vancura, T. Ihn, S. Broderick, K. Ensslin, W. Wegscheider, M. Bichler, Phys. Rev. B 62 (2000) 5074.
[11] A. Matulis, F.M. Peeters, P. Vasilopoulus, Phys. Rev. Lett. 72 (1994) 1518.
[12] G. Papp, F.M. Peeters, Appl. Phys. Lett. 78 (2001) 2184;
G. Papp, F.M. Peeters, Appl. Phys. Lett. 79 (2001) 3198.
[13] M.W. Lu, Solid State Commun. 134 (2005) 683;
M.W. Lu, Appl. Surf. Sci. 252 (2005) 1747.
[14] M. Büttiker, Phys. Rev. Lett. 57 (1986) 1761.